BIOCHEMISTRY
including biophysical chemistry & molecular biology

Article

pubs.acs.org/biochemistry

Interplay of Specific Trans- and Juxtamembrane Interfaces in Plexin A3 Dimerization and Signal Transduction

Rachael Barton,[†] Pouyan Khakbaz,[‖] Indrani Bera,[‖] Jeffery B. Klauda,[‖,⊥] M. Kathryn Iovine,[‡] and Bryan W. Berger*[,†,§]

[†]Department of Chemical and Biomolecular Engineering, Lehigh University, Bethlehem, Pennsylvania 18015, United States
[‡]Department of Biological Sciences, Lehigh University, Bethlehem, Pennsylvania 18015, United States
[§]Program in Bioengineering, Lehigh University, Bethlehem, Pennsylvania 18015, United States
[‖]Department of Chemical and Biomolecular Engineering, University of Maryland, College Park, Maryland 20742, United States
[⊥]Biophysics Program, University of Maryland, College Park, Maryland 20742-2431, United States

Supporting Information

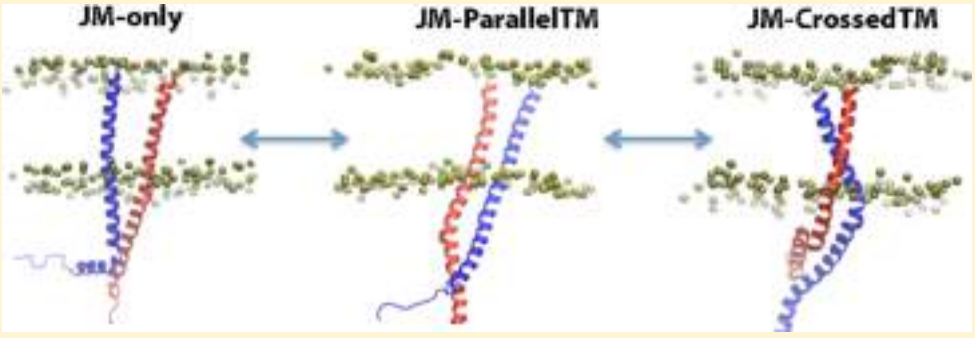

ABSTRACT: Plexins are transmembrane proteins that serve as guidance receptors during angiogenesis, lymphangiogenesis, neuronal development, and zebrafish fin regeneration, with a putative role in cancer metastasis. Receptor dimerization or clustering, induced by extracellular ligand binding but modulated in part by the plexin transmembrane (TM) and juxtamembrane (JM) domains, is thought to drive plexin activity. Previous studies indicate that isolated plexin TM domains interact through a conserved, small-x3-small packing motif, and the cytosolic JM region interacts through a hydrophobic heptad repeat; however, the roles and interplay of these regions in plexin signal transduction remain unclear. Using an integrated experimental and simulation approach, we find disruption of the small-x_3-small motifs in the *Danio rerio* Plexin A3 TM domain enhances dimerization of the TM−JM domain by enhancing JM-mediated dimerization. Furthermore, mutations of the cytosolic JM heptad repeat that disrupt dimerization do so even in the presence of TM domain mutations. However, mutations to the small-x_3-small TM interfaces also disrupt Plexin A3 signaling in a zebrafish axonal guidance assay, indicating the importance of this TM interface in signal transduction. Collectively, our experimental and simulation results demonstrate that multiple TM and JM interfaces exist in the Plexin A3 homodimer, and these interfaces independently regulate dimerization that is important in Plexin A3 signal transduction.

Plexins (plxns) make up a group of type I transmembrane (TM) receptors involved in the guidance of neurons and vascular and lymphatic vessels during development as well as zebrafish fin regeneration.[1−7] Plxns also serve a putative role in cancer metastasis, with altered expression levels or mutations to plxns observed in melanomas and breast, lung, pancreatic, and prostate cancers.[8−11] Investigations with plxns' semaphorin (sema) ligands and neuropilin (nrp) coreceptors have also implicated the plxn-nrp-sema pathway as being influential in cancer metastasis, with overexpression of SEMA3F inhibiting cancer metastasis in a mouse melanoma model.[4,11] As such, understanding the mechanisms necessary for activation of the plxn-nrp-sema signaling pathway might provide insight into the design of novel therapeutics as well as their role in a myriad of developmental processes.

Plxns contain an extracellular domain involved in ligand binding, a glycine-rich single-span TM domain, and a cytosolic domain (CYTO) involved in signal transduction.[1,2,4,12,13] Activity is characterized by CYTO GTPase-activating protein (GAP) activity and Rho GTPase binding leading to direct or indirect RhoA activation.[3,14−16] An early immunohistological observation that NRP1 and PLXNA1 cluster in regions of high local concentration upon SEMA3A addition in a chick dorsal

Received: May 22, 2016
Revised: August 10, 2016
Published: August 10, 2016

DOI: 10.1021/acs.biochem.6b00517
Biochemistry 2016, 55, 4928−4938

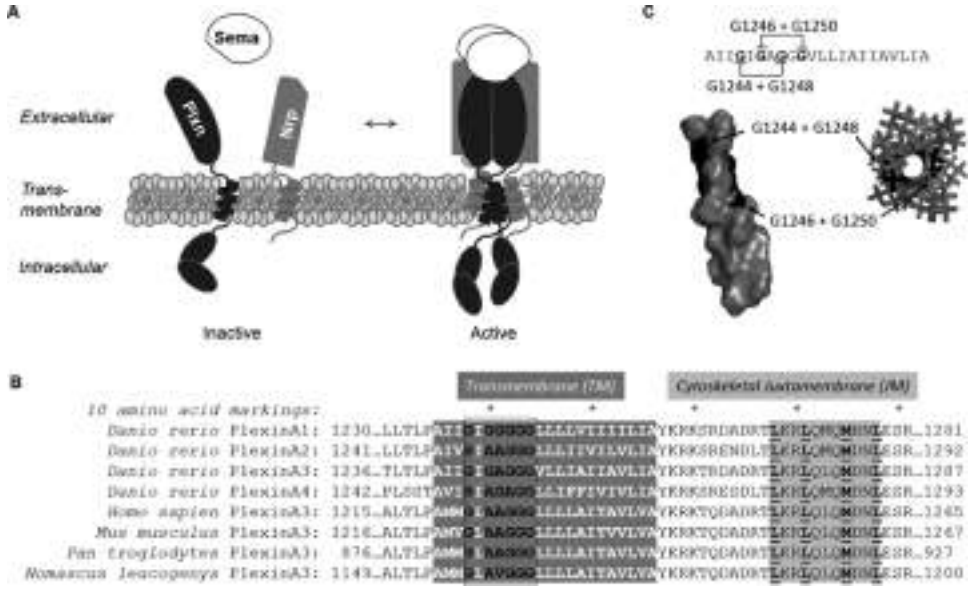

Figure 1. Plexin transmembrane and juxtamembrane domains contribute to receptor clustering and activation. (A) Extracellular binding of a semaphorin ligand (Sema) to plexin (Plxn) and neuropilin (Nrp) leads to receptor clustering and activation. (B) A small amino acid-rich region in the transmembrane domain and a cytosolic juxtamembrane heptad repeat are conserved across class A plexins and postulated to modulate homooligomerization. (C) Primary sequence analysis of the glycine-rich *Danio rerio* Plexin A3 transmembrane domain reveals two interfaces capable of participating in small-x_3-small packing motifs. Structural representation of the Plexin A3 transmembrane domain was generated using the asymmetric E_z-*3D* Potential Finder.

root ganglion collapse assay led to the premise that receptor dimerization or clustering confers activity.[2] Indeed, a RapGAP activity assay on purified CYTO domains of *Mus musculus* PLXNA1, PLXNA2, PLXNA4, and PLXNC1 CYTO suggests plxn CYTO domains dimerized through N-terminal fusions exhibit enhanced activity over the monomeric CYTO domains.[16]

Purified murine PLXNA2 extracellular domains and murine PLXNA1 and PLXNA3 and human PLXNB1 CYTO domains exhibit only weak homomeric tendencies in solution.[5,14−17] Removal of the murine PLXNA1 sema-binding domain or extracellular domain confers sema- and nrp-independent collapse activity in a COS-7 growth cone model; this indicates that PLXNA1 exists in an autoinhibited conformation and that in the absence of the sema-binding domain, the PLXNA1 TM + CYTO is sufficient for receptor activation.[12] Expression of the mouse PLXNA1 CYTO domain alone or with a myristoylation signal fails to induce collapse, though replacement of the human PLXNB1 TM domain with a membrane-anchored CD2 fusion followed by cross-linking permits cellular contraction.[12,18,19] Collectively, this previous membrane-anchored plxn clustering is important for activity, and the TM−JM regions exhibit an inherent tendency to promote plxn homooligomerization (Figure 1A).

Previous studies indicate a heptad repeat in the CYTO juxtamembrane region (JM) modulates homomeric interactions in the full-length receptor, with mutations to the JM of *Drosophila* PLXNA and *Danio rerio* PlxnA3 showing only partial activity in axonal guidance assays.[14,20] Additionally, the human PLXNA1 TM domain alone exhibits a weak tendency to dimerize in a bacterial adenylate cyclase two-hybrid assay.[13,21] Coarse-grained molecular dynamics simulations of the isolated human PLXNA1 TM domain suggest a glycine-rich segment in the TM region largely conserved across class A plxns may modulate human PLXNA1 homomeric interactions (Figure 1C).[13] In particular, this conserved glycine-rich region contains two motifs capable of packing via small-x_3-small interfaces.[13] The small-x_3-small motif is a highly conserved sequence structure motif overrepresented in a wide range of helical TM protein dimers such as glycophorin A and the plexin coreceptor NRP1, in which small residues such as glycine, serine, and alanine are placed along one face of the TM helix, creating a specific, ridge-and-groove packing structure that contributes to dimer stability.[21−23] A similar series of interfaces is also present in the *D. rerio* PlxnA3 TM domain (Figure 1B), suggesting a role in dimerization. However, the relative importance of TM versus JM and the interrelationship between TM and JM interactions in PlxnA3 dimerization and signal transduction remain open questions.

In this study, we examine the role of the glycine-rich region of the *D. rerio* PlxnA3 TM domain in homodimerization as well as the interplay of TM and JM interactions in PlxnA3 homodimerization and signal transduction. Interestingly, we find disruption of the small-x_3-small TM interface through glycine-to-leucine mutations enhances, rather than diminishes, dimerization of the TM−JM domain. Similarly, extension of the small-x_3-small interfaces through introduction of additional on-interface glycines disrupts, rather than enhances, dimerization. However, mutations to the JM heptad repeat that enhance or diminish dimerization do so even in the presence of TM domain small-x_3-small mutations, suggesting the TM dimer interface is distinct from that of the JM, and the two work in opposition to one another; in other words, the TM small-x_3-small interfaces inhibit JM-mediated TM−JM dimerization. CG- and AA-MD also reveal an interplay between TM and JM interactions during dimerization. In a zebrafish axonal guidance assay using *sidetracked* (*set*) zebrafish embryos, which exhibit ectopic motor neuron exit points due to a truncation in the *plxnA3* gene,[24,25] mutations to the small-x_3-small interfaces result in nonfunctional (mutation G1246L/G1250L) or only partially functional (mutation G1244L/G1248L) PlxnA3. Collectively, our results demonstrate multiple distinct, func-

DOI: 10.1021/acs.biochem.6b00517
Biochemistry 2016, 55, 4928−4938

tionally important interfaces exist in the PlxnA3 receptor TM and JM that regulate PlxnA3 signaling.

EXPERIMENTAL PROCEDURES

Homology Modeling. A model of the *D. rerio* PlxnA3 transmembrane domain (amino acids 1241−1262 of NCB accession number BAF81998.1) (Figure 1C) was generated using the asymmetric E_z-*3D* Potential Finder.[26]

Plasmids. Cloning for full-length wild-type (WT) *D. rerio plxnA3* in pcDNA3.1/V5-His-TOPO and the *plxnA3* TM and JM domains (amino acids 1241−1314 of NCB accession number BAF81998.1) in pAraTM was previously described.[20] Mutations were introduced using the QuikChange II Site-Directed Mutagenesis Kit (Agilent).

AraTM Assay. AraTM measurements and analyses were performed as previously described.[20,27] Briefly, electrically competent SB1676 cells were cotransformed with pAraGFP and the pAraTM construct of interest via electroporation. The transformed cells were grown in selective lysogeny broth (Lennox) medium (LB) overnight, and glycerol stocks were made from the cultures. Cultures for measurements (four per experimental round) were started from these glycerol stocks and allowed to grow 16−24 h in selective LB, at which time fluorescence (485 nm excitation, 530 nm emission) and absorbance (560 nm) measurements were taken for each culture (and 5-fold serial dilutions of each culture) using a Tecan Infinite F200 multiwell plate reader. Results are reported as the average percent change in the slope of fluorescence versus absorbance from WT from three rounds of experiments, with error bars indicating the standard error of the samples plus the standard error of WT samples analyzed in parallel. Expression and orientation in the membrane were confirmed by Western blotting and maltose complementation tests, respectively (Figure S1).

Zebrafish Care and Embryo Injections. The *set* zebrafish line, provided by M. Granato (University of Pennsylvania, Philadelphia, PA), was used for this study.[24,25] Care for parental zebrafish was previously described.[20] Husbandry occurred between adult heterozygous or homozygous *plxna3*/+ zebrafish. This study did not require animal sacrifice. Generation of mutant *plxnA3* RNA, injection into embryos, embryo processing (fixation, staining, imaging, and genotyping), and *set* phenotype classification requirements were as previously described.[20] We used previously reported values for the occurrence of the *set* phenotype with WT *plxnA3* RNA injections or uninjected *set* zebrafish embryos[20] for our statistical analyses.

Coarse-Grained Molecular Dynamics (CG-MD). Molecular dynamics studies were performed on the wild-type structures of Plexin A3 and two mutants to identify the effect of mutations on the dimerization of TM and JM regions. The first mutation was M1281F, and the second mutation was L1252G/I1254G. The initial structure consisting of two monomers each having 70 residues (residues 1240−1310) was derived from homology modeling using MODELLER; the initial structure of the Plexin A3 TM region was generated using the asymmetric E_z-*3D* Potential Finder and integrated into a homology model for the TM−JM region using the crystal structure of the Plexin A3 intracellular domain.[14] A similar approach was also described recently for developing TM−JM models for Plexin B1 and C1.[28]

The initial conformations were built using CHARMM-GUI *Martini Bilayer Maker*[29−31] with the separation of the two TM helices by having the closest contact of ∼0.8 nm. The Martini force field with nonpolarizable water (Martini 2.2[32,33]) was used with explicit solvent, and a bilayer of 1-palmitoyl-2-oleoyl-*sn*-glycero-3-phosphocholine (POPC) lipids with 100 lipids in each leaflet was added for simulations. The systems were neutralized by adding two Na^+ ions, which may slightly increase electrostatic interactions in our MD simulations compared to higher-ionic strength solutions. MD simulations were conducted using GROMACS 5.0.4.[34,35] The systems were energy minimized using 5000 steps of a steepest descent algorithm followed by equilibration runs. Ten microsecond production runs (unscaled time) were performed in the constant molecule, pressure, and temperature (*NPT*) ensemble at 310 K and 1 bar. For pressure coupling, the Berendsen method[36] was used with semi-isotropic scaling at a pressure of 1 bar. Shift[37] was used for both electrostatics and van der Waals calculations with forces decaying between 9 and 12 Å. A 25 fs time step was used, and coordinates were saved every 125 ps. All runs were replicated thrice to avoid biased results. Average distances between each residue of one monomer and all other residues in the other monomer were calculated using *gmx distance*. Inter-residue contact maps were generated using MATLAB.

All-Atom MD (AA-MD). Plexin A3 dimer structures obtained from CG simulations were used as initial configurations of AA-MD simulations. CG to AA conversion was conducted using a backmapping tool that uses a library of mapping definitions that encode geometrical reconstruction.[38] Dimers were placed in a POPC explicit bilayer using the CHARMM-GUI *Membrane Builder*;[39−42] 100 lipids were selected per leaflet, and a 15 Å layer of water was used as a buffer on the top and bottom of the system (including the peptide). The NAMD simulation package[43] was used to run all simulations. The temperature and pressure were fixed at 310.15 K and 1 bar, respectively. The Lennard-Jones potential was used to describe van der Waals interactions, and a force-based switching function in the range of 8−12 Å was chosen.[44] Hydrogen atoms were constrained by using the RATTLE algorithm.[45] Langevin dynamics maintained the temperature, and the Nosé−Hoover Langevin piston algorithm[46,47] was used to maintain the pressure. Three replicates using different initial CG structures were performed for wild-type and second mutation conformations, while two runs were performed for the first mutant simulation. Simulations were run for 300 ns; the time step was 2 fs, and two or three replicas were run to provide better statistics with dimerization. The CHARMM36 (C36) force field was used for the protein and lipids[48,49] and TIP3P for water.[50,51] CHARMM[31,52] was used to calculate the distances between residues, and then contact maps were generated using MATLAB. All images were made using visual molecular dynamics (VMD).[53]

RESULTS

Transmembrane Glycines Modulate PlxnA3 Homodimerization. The *D. rerio* PlxnA3 TM domain contains a glycine-rich region [G_{1244}IGAGGG$_{1250}$ (Figure 1C)] with two putative interfaces capable of promoting homodimerization via small-x_3-small packing motifs (G1244+G1248 and G1246+G1250). Previous coarse-grained molecular dynamics simulations implied the homologous interfaces in the human PLXNA1 TM domain contribute to dimerization of the isolated TM domain.[13] To investigate the role of TM glycines in PlxnA3 TM and JM homodimerization, we employed site-directed mutagenesis in conjunction with the AraTM assay.[27] In this

DOI: 10.1021/acs.biochem.6b00517
Biochemistry 2016, 55, 4928−4938

assay, the TM domain of interest is expressed as an AraC fusion. Dimerization induced by TM homomeric interactions forms a functional AraC transcription factor, which in turn drives transcription of green fluorescent protein (GFP) regulated by a P_{BAD} promoter. Hence, AraTM cultures expressing TM domains with a stronger propensity to dimerize will exhibit an increased intensity of the GFP signal versus those of weaker dimer constructs for the same cell density.[27]

Our AraTM results illustrate that glycine-to-leucine mutations disrupting the small-x_3-small packing interfaces in the glycine-rich PlxnA3 TM domain actually enhance TM−JM dimerization, either as single-point mutations to a given interface [G1244L, G1246L, G1248L, and G1250L (Figure 2A)], double mutations to eliminate an interface [G1244L/G1248L and G1246L/G1250L (Figure 2B)], or triple mutations to disrupt both small-x_3-small interfaces [G1244L/G1246L/G1250L and G1246L/G1248L/G1250L (Figure 2B)]. Furthermore, extension of the small-x_3-small motif by placing additional glycines on either interface (L1252G and I1254G) disrupts, rather than enhances, TM−JM dimerization (Figure 2A). Collectively, our results indicate small-x_3-small interfaces in the PlxnA3 TM domain negatively regulate TM−JM dimerization (Figure 1).

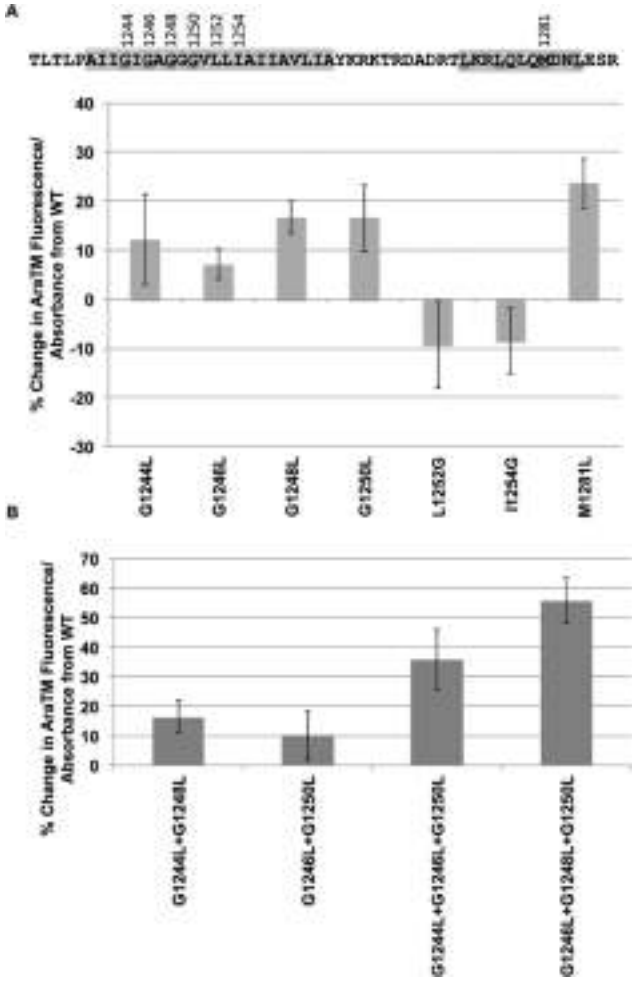

Figure 2. (A) Disruption of small-x_3-small interfaces in the Plexin A3 TM domain via point mutations enhances TM and JM dimerization in the AraTM assay. Similarly, extension of the small-x_3-small interfaces via introduction of glycines disrupts TM and JM dimerization. (B) Double and triple mutations disrupting the Plexin A3 TM small-x_3-small interfaces enhance dimerization of the TM and JM in the AraTM assay. Error bars indicate the standard error as determined from 12 replicates collected over a minimum of three experiments. Data for M1281L were adapted from ref 20.

TM and JM Interfaces Independently Regulate PlxnA3 Homodimerization. Previous work has demonstrated a specific heptad repeat in the PlxnA3 JM domain contributes to receptor TM−JM dimerization, with residue M1281 within this heptad repeat acting as a dimerization "switch", in which mutation M1281F disrupts dimerization by destabilizing packing in the hydrophobic core of the JM heptad repeat and mutation M1281L enhances dimerization by enhancing packing in the hydrophobic core of the JM heptad repeat.[20] To determine how interactions in the JM interface influence TM−JM dimerization, and what role these interactions play in the observed increase in the level of TM−JM dimerization caused by disruption of the TM small-x_3-small interface, we compared effects of key mutations in the TM region that enhance TM−JM dimerization to mutations in the JM shown previously to enhance or diminish TM−JM dimerization.

As shown in Figure 3, mutations to the JM region are dominant versus those in the TM domain; regardless of

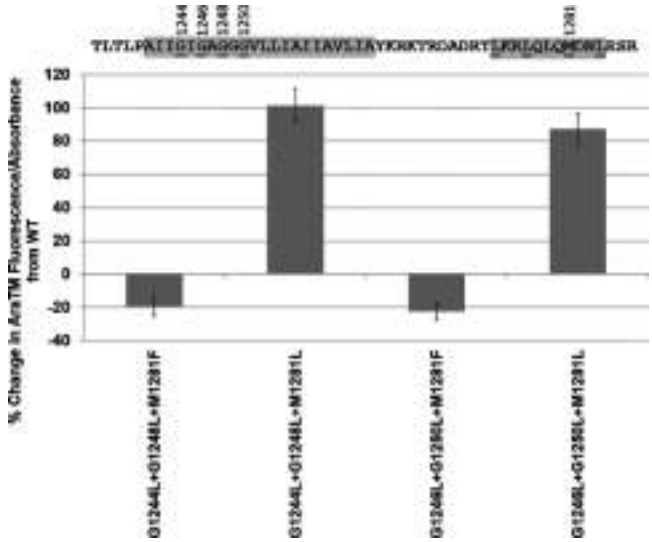

Figure 3. Mutations to the Plexin A3 JM domain dominate dimerization tendencies of the TM and JM in the AraTM assay. Error bars indicate the standard error as determined from 12 replicates collected over a minimum of three experiments.

mutations to the two putative small-x_3-small interfaces of the TM, all of which enhance dimerization, mutations made in conjunction with the disruptive M1281F JM mutation weaken TM−JM dimerization, whereas mutations made in conjunction the enhancing M1281L JM mutation enhance TM−JM dimerization. Furthermore, the enhancements to dimerization through mutation of either of the two small-x_3-small interfaces (Figure 2) or M1281L[20] are nonadditive; mutation of each domain individually enhances dimerization by less than 25% relative to wild-type dimerization, compared to more than 80% observed with mutation to both the TM and the JM (Figure 3). This suggests the TM small-x_3-small interfaces serve as competitive TM−JM dimers to those formed by the JM heptad repeat interface. Thus, enhancement of the small-x_3-small dimerization interface via introduction of additional on-interface glycines [L1252G and I1254G (Figure 2A)]

DOI: 10.1021/acs.biochem.6b00517
Biochemistry 2016, 55, 4928−4938

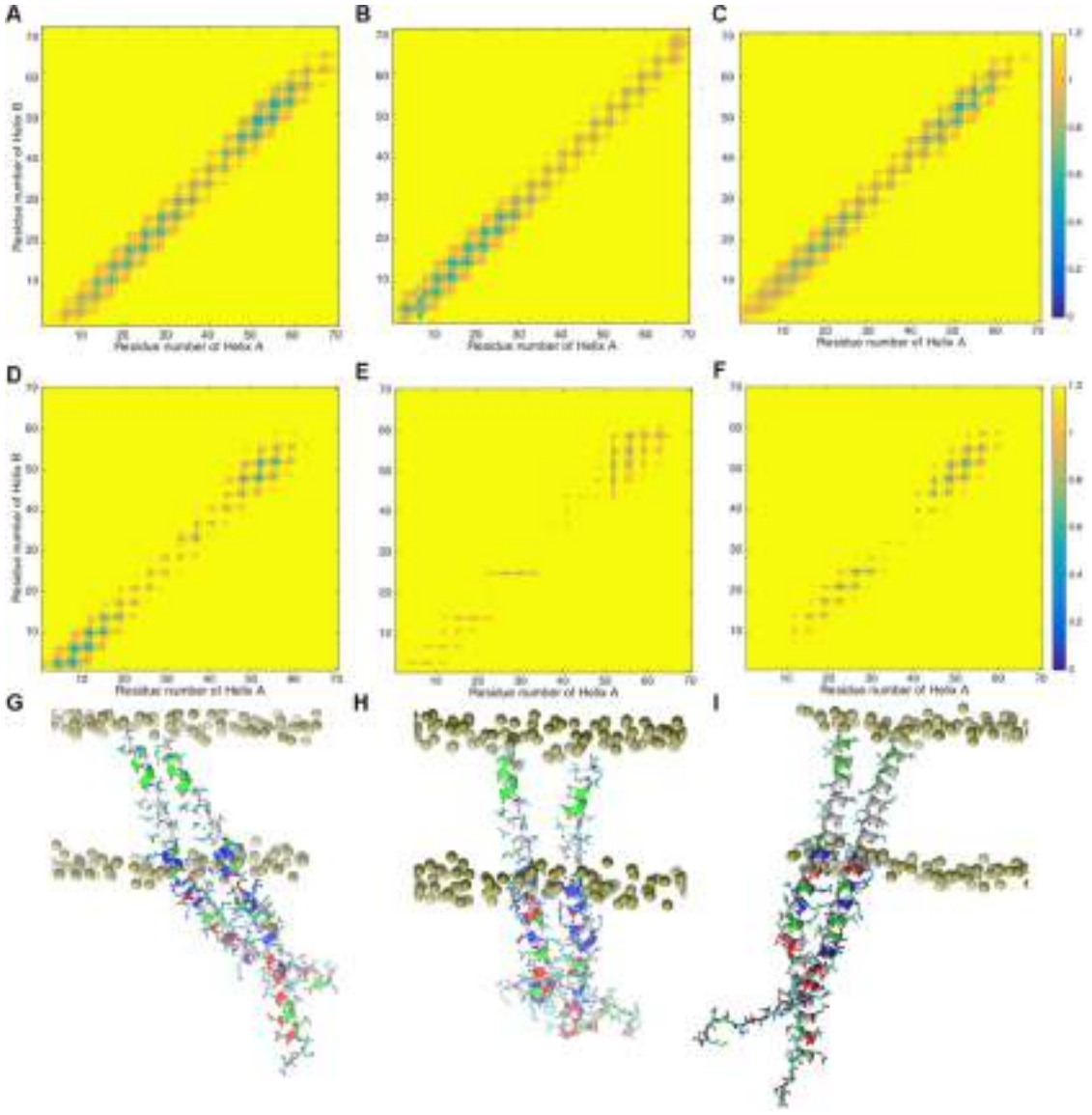

Figure 4. Results from CG- and AA-MD for the wild-type Plexin A3 TM−JM domain. The top three panels are contact maps for three CG runs (A−C) with the residue numbers starting at 1240 in full-length protein numbering. The middle three panels (D−F) are for the respective AA-MD simulations that correspond to the CG starting configurations. The color bars are in nanometers, and maps are averages over the last 2.5 μs and 100 ns of simulation for CG- and AA-MD, respectively. End snapshots from the 300 ns AA-MD runs are shown in the bottom panels, with nonpolar, polar, acidic, and basic residues colored white, green, red, and blue, respectively. The phosphate atoms are colored gold.

strengthens the TM dimer and pulls the TM−JM interface away from the JM dimer, whereas disruption or removal of the small-x_3-small interfaces through glycine-to-leucine mutations (Figure 2) removes the TM dimer competition and strengthens the JM dimer. Collectively, our results are consistent with a model in which TM dimerization and JM dimerization are competitive, with each providing a distinct interface capable of forming a TM−JM dimer (Figure 3).

Simulations of the Wild-Type and Mutant TM−JM Interface Illustrate the Diversity of Specific TM and JM Interactions That Contribute to the Dimeric States Formed. As described in Experimental Procedures, the homology-modeled Plexin A3 TM−JM domains were separated initially in a POPC bilayer and CG simulations with the MARTINI force field were performed. In <100 ns, the dimers associated from their initial separation and remained tightly packed for the 10 μs simulation. The contact maps (Figure 4A−C) and snapshots (Figure S2) show some variations between replicas but consistently show an interacting TM and JM domain. Replica 1 (Figure 4A) shows weaker TM domain packing and a slip in dimer interaction with an off diagonal contact; in other words, a residue of Plexin A3 TM helix 1 is not in contact with the same residue on the second Plexin A3 TM helix. The JM domain in replica 2 (Figure 4B) is interacting more weakly, but the TM domain associates strongly. The overall dimer character of replica 3 (Figure 4C) is similar to that of replica 1, but the contact maps are on the diagonal; in other words, a residue on Plexin A3 TM helix 1 is in close contact with the same residue on the second Plexin A3 TM helix. There is a slightly weaker interaction for the TM domain residues from position 1240 to 1255 for replica 3. On the basis of these CG-MD simulations, there are slight changes in the strength of the TM and JM interactions, but examples of complete dissociation of these domains are lacking, except the

DOI: 10.1021/acs.biochem.6b00517
Biochemistry 2016, 55, 4928−4938

end of the TM region. Thus, for the wild-type Plexin A3 TM−JM interface, multiple, independent TM and JM interactions, each of which contain a specific interface, are consistently observed; both the TM and JM interfaces contribute to a stable Plexin A3 TM−JM homodimer.

Because the MARTINI CG-MD simulations lack the ability to change secondary structure from the initial model, the primary structure was fixed as a helix for the TM−JM region based on previous crystal structures of the JM region. To relax this constraint, end configurations form the 10 μs simulations were used to set up and run 300 ns AA MD. Our multiscale approach allows for sampling at the CG level to overcome the long times needed for association and rotation that tend to occur on a microsecond time scale.[54] Dimerization motifs that are not observed in the CG-MD will require sampling with AA-MD that might be beyond our AA-MD time scale. However, on the basis of our AA MD simulations, this 300 ns time scale is sufficient to observe helix shifts, small rotations, and helix crossing that was not observed at the CG level (see below).

The results of AA-MD simulations show more diversity in TM−JM association for Plexin A3 (Figure 5D−I and Figure S3). Specifically, replica 1 (Figure 5D,G) shows a strongly tilted helix in the membrane with weakened association in the cytoplasmic leaflet; the main association is in the G-x_3-G motif region of the TM domain, which is stable for the last 100 ns based on probability distance plots for the Gly1248 distance (Figure S4D). Also, consistently across independent replicas, there is a tendency to form a cross JM motif interaction. Replica 2 completely separates in the TM but maintains JM interaction to a lesser extent (Figure 5E,H). Replica 3 has no association in the extracellular half of the TM domain but enhanced association for the cytoplasmic half (Figure 5F,I); a similar JM association is observed for replica 1, as well. The stabilization of this JM region is promoted by hydrogen bonding between R1287 (from helix 1) and E1285 (helix 2) (Figure 6A), which varies in its stability during the course of the last 100 ns (Figure S4A). It is clear that even with the JM region there is some plasticity of homodimerization structures.

Overall, these wild-type AA-MD results suggest a strongly interacting JM region and a weaker interacting TM region with multiple dimeric conformations for Plexin A3 (Figure S3). This weaker TM region interaction may be the result of not including residues beyond the TM region of the N-terminus, which was shown to be important in other proteins with a G-x_3-G motif.[28,55] However, the lack of these residues does not preclude stabilization of TM-associated motifs observed for the wild type and mutants (see below).

MD simulations were performed for the disruptive JM mutant M1281F to probe how this nonpolar, aromatic substitution within the hydrophobic JM coiled-coil motif influences JM association. From the CG-MD of the wild type, the strongest JM association was with JM residues 1285−1300 (Figure 4A−F). However, mutant M1281F abolishes this preference and moderately promotes the association for JM residues at positions 1300 and above (Figure 5A); this is consistent with the expected result that removing hydrophobic residues in the core of the coiled coil destabilizes JM association. Furthermore, the M1281F mutant also appears to enhance TM region association, again consistent with a model in which loss of JM association can be compensated by independent TM domain interactions.

The enhancement of TM domain interactions at the expense of weakened JM interactions is in conflict with our AA-MD

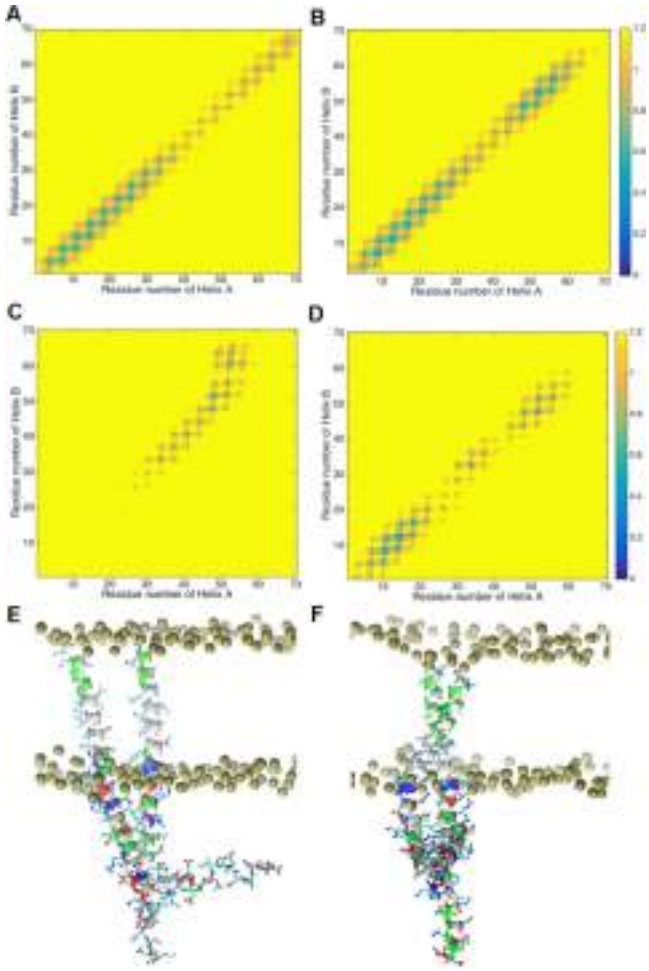

Figure 5. Results from CG- and AA-MD for the mutant Plexin A3 TM−JM domain. The top two panels are sample CG-MD contact maps with the residue numbers starting at 1240 in full-length protein numbering. The middle two panels are contact maps for AA-MD. Panels A, C, and E show data for the M1281F mutant, and panels B, D, and F show data for the L1252G/I1254G double mutant. The color bars are in nanometers, and maps are averages over the last 2.5 μs and 100 ns of simulation for the CG- and AA-MD, respectively. End snapshots from the 300 ns AA-MD runs are shown in the bottom panels with nonpolar, polar, acidic, and basic residues colored white, green, red, and blue, respectively. The phosphate atoms are colored gold.

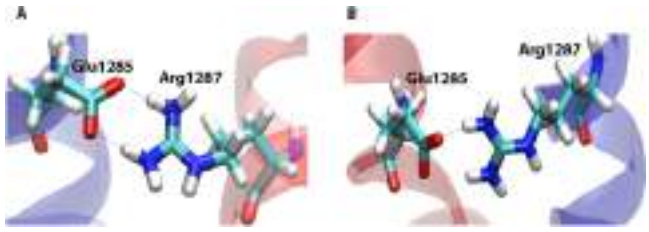

Figure 6. (A) Wild-type simulation snapshot (replica 1). (B) M1281F mutant simulation snapshot (replica 2). JM association due to hydrogen bonding between Glu1285 and Arg1287.

(Figure 5C and E), which shows an enhanced interaction for JM residues at positions 1300 and above (for one helix) and a slight decrease in the residues near mutation M1281F, yet a complete loss of interactions in the TM region. This result can also be seen for the second replicate of this mutation (Figures

DOI: 10.1021/acs.biochem.6b00517
Biochemistry 2016, 55, 4928−4938

S5 and S6). This is likely due to the weaker interaction in the TM region as well as the inability of the CG MARTINI model to kink the helices, thus maintaining an extended, rodlike structure that promotes helix association in the TM domain. Although hydrogen bonding between R1287 and E1285 exists (Figure 6B), this is less stable during the course of the simulation than in the wild type (Figure S4A,B). Overall, these results indicate that M1281F causes a specific disruption of the JM coiled-coil dimer, resulting in a weaker association with a variable and weaker TM association observed.

Simulations were performed for the TM double mutant L1252G/I1254G, which places an additional glycine in registry with each of the small-x_3-small motifs (G1244 and G1248, and G1246 and G1250) present in Plexin A3. Thus, this TM double mutant is hypothesized to be a mutant that enhances TM-mediated homodimerization. For CG-MD, there was a slight reduction in the level of JM domain association, excluding replica 1 (data not shown). However, with this double mutant, there is an enhanced contact for TM residues 1240−1255, which encompasses the region containing both small-x_3-small motifs.

The first replicate of AA-MD of double mutant L1252G/I1254G shows a more crossed TM and JM motif (Figure 5F) with strong association in the TM region (Figure 5D). The G1248 within the extracellular leaflet shows weakened interaction compared to that of the wild type (Figure S4D,F). However, for replica 1, the two additional glycines promote interactions between G1252 and G1254 (Figure S7A−D) to stabilize this crossed TM motif near the center of the bilayer instead of near the extracellular space (Figure 5F). This crossed TM motif results in a more upright dimer compared to those observed in the wild type (Figure 4G−I). The wild type has a slipped registry in cross TM interaction compared to the more aligned registry for the double mutant and its crossed motif (Figure S7A−D). The shortest contact for the wild type is between residues G1250 and V1251, while for the double mutant, this contact is between the mutated residues (Figure S7E,F). The stabilization of the TM in replica 1 influences the JM motif in that the R1287···E1285 hydrogen bond is destabilized. Replicas 2 and 3 resulted in weaker interaction in the JM domain with a more parallel motif and a similar motif in the TM region (Figures S4F, S8, and S9). Thus, these results indicate mutations L1252G and I1254G that enhance TM small-x_3-small packing motifs do enhance overall TM-mediated homodimerization relative to that of the wild type and can do so at the expense of the JM coiled-coil homodimer.

Glycines in the Transmembrane Domain Modulate PlxnA3 Function in a Zebrafish Axonal Guidance Assay. Zebrafish embryos failing to express membrane-anchored PlxnA3, such as homozygous *sidetracked* (*set*) zebrafish embryos, exhibit anomalous motor neuron patterning, with motor neurons exhibiting atypical branching and ectopic exit points from the spinal cord (Figure 7).[24,58] Previous studies demonstrated that *set* embryos injected with WT *plxnA3* RNA rescue the *set* phenotypes, showing significantly fewer ectopic motor neuron exit points than uninjected *set* embryos do; a representative image of the *set* phenotype rescue is provided (Figure 7).[20] To understand the functional effects of PlxnA3 TM mutations, we tested the ability of mutant forms of PlxnA3 to also rescue the set phenotypes. This was accomplished by injecting *set* embryos while in the single-cell stage with mutant *plxnA3* RNA. Motor neurons were evaluated for ectopic exit points at 24 h postfertilization (Table 1). Comparisons to WT *plxnA3* RNA-injected and uninjected *set* embryos were made on the basis of previous studies.[20] We found in this previous study that the background of the *set* phenotypes in uninjected *set* embryos is 80%, compared with 36% when WT *plxnA3* RNA is injected.

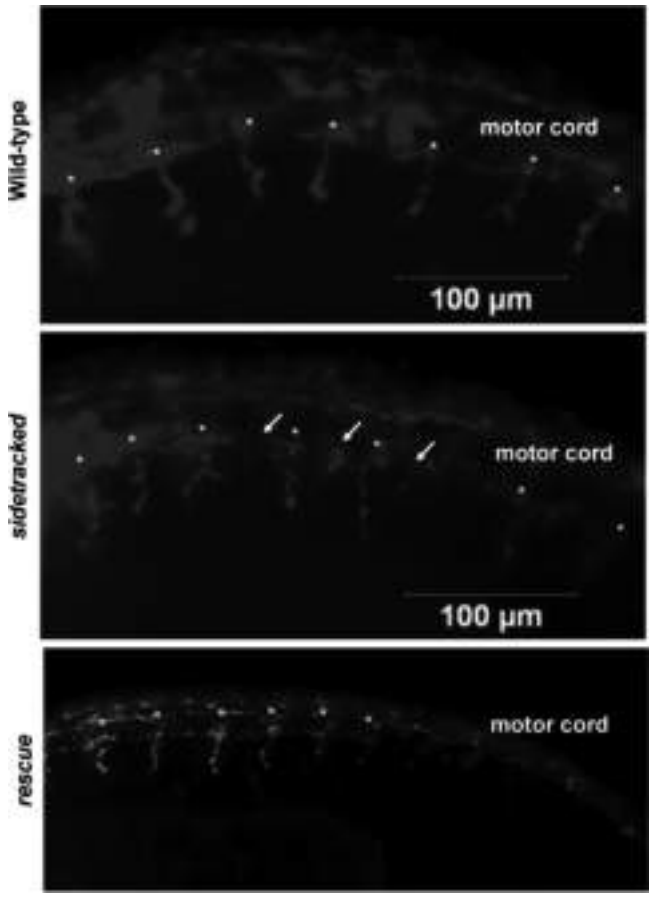

Figure 7. Embryos with the *sidetracked* phenotype exhibit ectopic motoneuron exit points (arrows) vs wild-type zebrafish (wild-type) and *sidetracked* phenotype rescued using WT *plxnA3* RNA (rescue). Endogenous motoneuron exit points are marked with an asterisk. Embryos were 24 h postfertilization at the time of fixation and are oriented anterior to posterior (left to right, respectively).

Table 1. Percentages of Homozygous *sidetracked* Embryos Exhibiting Phenotypes[a]

type of RNA injection	no. of embryos evaluated	percentage of embryos exhibiting the *sidetracked* phenotype	*p* value compared to wild-type *plxnA3* with RNA injected
G1244L/G1248L	13	62	0.2
G1246L/G1250L	19	74	0.03
M1281L	12	50	0.07

[a] *p* values were computed using a Fisher's Exact Test and previously reported values for uninjected and WT embryos.[20] Data for M1281L were taken from ref 20.

Injection of *set* embryos with G1246L/G1250L *plxnA3* RNA results in significantly more embryos than WT *plxnA3* RNA-injected embryos exhibiting the *set* phenotype [74% of embryos exhibited the *set* phenotype; $p < 0.05$ relative to WT as determined by a Fisher's Exact Test (FET)]. This demonstrates

DOI: 10.1021/acs.biochem.6b00517
Biochemistry 2016, 55, 4928−4938

a failure of the G1246L and G1250L mutations to rescue PlxnA3 function. In contrast, injection of G1244L/G1248L *plxnA3* RNA partially rescues the *set* phenotype (62% of embryos exhibited the *set* phenotype; $p > 0.05$ compared to 80% of embryos exhibiting the *set* phenotype in uninjected *set* embryos as determined by a FET). Both of these mutations enhanced dimerization of the TM and JM domains in the AraTM assay (Figure 2). Thus, our results are broadly consistent with a model in which destabilizing the TM dimer facilitates formation of a stronger, nonfunctional JM dimer during PlxnA3-dependent signaling.

DISCUSSION

Previous studies suggest that plxn function depends on receptor clustering and that function and clustering are modulated by the TM and JM domains (Figure 1).[12,13,16,18−21,57] In this study, we demonstrate that glycine-to-leucine mutations disrupting putative small-x_3-small packing interfaces in the TM region of *D. rerio* PlxnA3 enhance dimerization of TM and JM domains in the AraTM assay (Figure 2). Similarly, extension of the small-x_3-small interfaces disrupts dimerization (Figure 2). Mutations to the previously established dimer interface in the PlxnA3 JM[20] dominate dimer formation of the TM and JM, with mutations to either TM small-x_3-small interface in conjunction with M1281F JM disrupting dimerization and mutations to the TM interfaces with M1281L JM enhancing dimerization (Figure 3). Functionally, disruption of the PlxnA3 TM interface fails to rescue WT motor neuron patterning in a zebrafish axonal guidance assay, with the G1244L/G1248L mutant exhibiting partial activity and the G1246L/G1250L mutant displaying no activity (Figure 7 and Table 1). Thus, our results point to a model for PlxnA3 dimerization in which the TM and JM both play important and independent roles in regulating signal transduction. A model in which both TM and JM interactions work independently is also supported by the CG-MD and AA-MD simulations for the Plexin A3 TM−JM interface presented in this study (Figures 4 and 5), in which consistently a coiled-coil JM interface and a small-x_3-small TM interface are observed for the homodimeric WT Plexin A3 TM−JM domain. A recent CG-MD simulation also suggests that the isolated human PLXNA1 TM domain undergoes homooligomerization via two putative small-x_3-small interfaces,[13] homologous to the *D. rerio* PlxnA3 interfaces of G1244 and G1248, and G1246 and G1250, identified in this study, although the role of the JM was not considered in the simulation. Additional work investigating the role of TM and JM interactions in Plexin B1 and C1 also provides insight into the diversity of TM and JM dimerization motifs; while both occur, there is a large degree of diversity in terms of cooperative versus competitive interactions involving both the conserved JM coiled coil and TM G-x_3-G motif.[28] Thus, the proposed interaction model from the PlxnA3 TM−JM interface is consistent with previous work regarding plexin TM domain dimerization, as well as with functional, biochemical, and simulation results regarding TM−JM dimerization. Furthermore, these results emphasize the importance of JM interactions in describing models for receptor TM−JM dimerization.

Typically, mutation of small-x_3-small interaction motifs disrupts dimerization, as has been shown with GpA and NRP1.[23,58] This motif promotes TM dimerization by providing a specific interface that is favorable to steric packing constraints as well as additional side chain associations.[22,59−61] For wild-type Plexin A3 (replica 2 in Figures 4B and 6), a specific interaction interface for the TM−JM heterodimer involving the G-x_3-G motif is observed based on CG-MD simulations. Hence, the result that mutations to the PlxnA3 TM small-x_3-small motifs enhance TM−JM dimerization is at first counterintuitive (Figure 2). However, the interplay of TM and JM interfaces as distinct dimers, but with both being significant in terms of promoting TM−JM dimerization, provides a model in which multiple, competitive dimeric states occur for the TM−JM region, each of which is important in negatively regulating signal transduction. This interplay is also observed in CG-MD wild-type Plexin A3, in which both specific TM (small-x_3-small) and JM (coiled-coil) interfaces are observed in the TM−JM dimer (Figure 4). In this sense, the proposed TM−JM model resembles a "push−pull" mechanism used in describing the competition between integrin homo- and heterodimerization. In the case of PlxnA3, the two states (TM dimer and JM dimer) are intrinsic to the receptor and in competition, with mutations that favor either of these interfaces "pulling" the receptor toward that interface and mutations that destabilize either of these interfaces "pushing" the TM−JM heterodimer toward the other interface. Our results suggest glycines in the TM domain contribute to dimers driven by small-x_3-small packing motifs that compete with JM-driven dimers, and this competition prevents strong JM dimerization. We observe a similar pattern of behavior for WT versus mutant TM−JM simulations (Figure 5) in which mutations that are disruptive to homodimerization in the JM (M1281F) or enhance homodimerization in the TM (L1252G/L1254G) do alter the configuration of the TM−JM heterodimer to promote switching between the two different interfaces. This mechanism likely contributes to class A plexin flexibility in coreceptor heterodimerization[4,13,21] as well as regulated switchability between active and inactive states.

Our study also indicates that PlxnA3 dimerization does not necessarily correlate with enhanced function (Figure 2 and Table 1), similar to previous results with mutations in the PlxnA3 JM domain.[20] Rather, an equilibrium between specific, dimeric conformations of the Plexin A3 TM−JM system participates in the regulation of Plexin A3 activity. The CG-MD results also indicate the likelihood of multiple, independent dimeric conformations occurring for the TM−JM heterodimer (Figure 4). Our results for PlxnA3 are similar to those of previous studies with ErbB2, for which dimerization is required, but not sufficient, for activity; replacement of the ErbB2 TM domain with the GpA TM domain, though dimerized through the GpA small-x_3-small motif, fails to elicit a transformation phenotype.[62] It is also analogous to the role of integrin TM domains in integrin activation,[63] in which the TM domain makes only a modest contribution to receptor dimerization, yet mutations to these TM interfaces have a significant impact on signal transduction (Table 1).

In summary, our AraTM results demonstrate that glycines in the *D. rerio* PlxnA3 TM domain modulate receptor homomeric interactions (Figure 2). In particular, small-x_3-small dimerization motifs in the TM domain compete with dimerization driven by the heptad repeat in the JM domain (Figure 1). As JM-driven dimerization predominates in the TM−JM system (Figure 3), mutation of the small-x_3-small interfaces results in overall enhancement of TM−JM dimerization. These interfaces both act competitively to regulate signaling, with the TM small-x_3-small interfaces exhibiting no or partial functionality in an embryonic zebrafish axonal guidance assay (Figure 7 and Table 1). Hence, the interplay of TM versus JM dimerization serves

DOI: 10.1021/acs.biochem.6b00517
Biochemistry 2016, 55, 4928−4938

as an important regulatory mechanism in PlxnA3 signal transduction (Figure 1). Recent structures of Plexin A1 and A2 ectodomains have suggested an autoinhibited confirmation of the ectodomain in which the cytosolic domains may be separated;[64] thus, the TM and JM regulatory roles described in this work may serve as additional mechanisms to inhibit or modulate signal transduction upon ligand binding. Given other receptors in which JM interactions independently, and often competitively, regulate transmembrane dimerization and signaling,[65−68] it will be interesting to see how other receptor systems couple TM and JM interactions to promote both homo- and heterodimerization as well as to regulate specificity versus signal transduction.

■ ASSOCIATED CONTENT

Supporting Information

The Supporting Information is available free of charge on the ACS Publications website at DOI: 10.1021/acs.biochem.6b00517.

One supplemental table and supplemental figures (PDF)

■ AUTHOR INFORMATION

Corresponding Author

*Department of Chemical and Biomolecular Engineering, Lehigh University, B320 Iacocca Hall, 111 Research Dr., Bethlehem, PA 18015. E-mail: berger@lehigh.edu. Phone: (610) 758-6837.

Funding

This work was supported by the Howard Hughes Medical Institute Biosystems Dynamics Summer Institute, the PA Research in Advanced Manufacturing Program, the Lehigh University Presidential Fellowship, National Institutes of Health Grant R03 HD070172 (M.K.I.) and National Science Foundation Grants CBET-1227924 (R.B. and B.W.B.) and MCB-1149187 (J.B.K., P.K., and I.B.).

Notes

The authors declare no competing financial interest.

■ ACKNOWLEDGMENTS

We thank Dr. Michael Granato (University of Pennsylvania) for his donation of the *sidetracked* zebrafish line and *D. rerio plxnA3* DNA template. We also thank Rebecca Bowman for care of the fish facility and Joyita Bhadra, Danica Palacio, Paige Dyrek, Pin-Chuan Su, and Diego Liriano for technical assistance. The following high-performance computational resources are acknowledged: Deepthought and Deepthought2 maintained by the Division of Information Technology at the University of Maryland and Maryland Advanced Research Computing Center (MARCC) managed by Johns Hopkins University and the University of Maryland.

■ ABBREVIATIONS

AA, all-atom; GC, coarse-grained; CYTO, cytosolic domain; FET, Fisher's Exact Test; GAP, GTPase-activating protein; GFP, green fluorescent protein; GpA, glycophorin A; JM, cytosolic juxtamembrane region; LB, lysogeny broth (Lennox) medium; MD, molecular dynamics; nrp, neuropilin; plxn, plexin; sema, semaphorin; *set*, *sidetracked*; TM, transmembrane; WT, wild type.

■ REFERENCES

(1) Tamagnone, L., Artigiani, S., Chen, H., He, Z., Ming, G. I., Song, H., Chedotal, A., Winberg, M. L., Goodman, C. S., Poo, M., Tessier-Lavigne, M., and Comoglio, P. M. (1999) Plexins are a large family of receptors for transmembrane, secreted, and GPI-anchored semaphorins in vertebrates. *Cell 99*, 71−80.

(2) Takahashi, T., Fournier, A., Nakamura, F., Wang, L. H., Murakami, Y., Kalb, R. G., Fujisawa, H., and Strittmatter, S. M. (1999) Plexin-neuropilin-1 complexes form functional semaphorin-3A receptors. *Cell 99*, 59−69.

(3) Negishi, M., Oinuma, I., and Katoh, H. (2005) Plexins: axon guidance and signal transduction. *Cell. Mol. Life Sci. 62*, 1363−1371.

(4) Kruger, R. P., Aurandt, J., and Guan, K. L. (2005) Semaphorins command cells to move. *Nat. Rev. Mol. Cell Biol. 6*, 789−800.

(5) Tong, Y., Hota, P. K., Penachioni, J. Y., Hamaneh, M. B., Kim, S., Alviani, R. S., Shen, L., He, H., Tempel, W., Tamagnone, L., Park, H. W., and Buck, M. (2009) Structure and function of the intracellular region of the plexin-b1 transmembrane receptor. *J. Biol. Chem. 284*, 35962−35972.

(6) Torres-Vazquez, J., Gitler, A. D., Fraser, S. D., Berk, J. D., Pham, V. N., Fishman, M. C., Childs, S., Epstein, J. A., and Weinstein, B. M. (2004) Semaphorin-plexin signaling guides patterning of the developing vasculature. *Dev. Cell 7*, 117−123.

(7) Ton, Q. V., and Kathryn Iovine, M. (2012) Semaphorin3d mediates Cx43-dependent phenotypes during fin regeneration. *Dev. Biol. 366*, 195−203.

(8) Balakrishnan, A., Penachioni, J. Y., Lamba, S., Bleeker, F. E., Zanon, C., Rodolfo, M., Vallacchi, V., Scarpa, A., Felicioni, L., Buck, M., Marchetti, A., Comoglio, P. M., Bardelli, A., and Tamagnone, L. (2009) Molecular profiling of the "plexinome" in melanoma and pancreatic cancer. *Hum. Mutat. 30*, 1167−1174.

(9) Wong, O. G., Nitkunan, T., Oinuma, I., Zhou, C., Blanc, V., Brown, R. S., Bott, S. R., Nariculam, J., Box, G., Munson, P., Constantinou, J., Feneley, M. R., Klocker, H., Eccles, S. A., Negishi, M., Freeman, A., Masters, J. R., and Williamson, M. (2007) Plexin-B1 mutations in prostate cancer. *Proc. Natl. Acad. Sci. U. S. A. 104*, 19040−19045.

(10) Staton, C. A., Shaw, L. A., Valluru, M., Hoh, L., Koay, I., Cross, S. S., Reed, M. W., and Brown, N. J. (2011) Expression of class 3 semaphorins and their receptors in human breast neoplasia. *Histopathology 59*, 274−282.

(11) Bielenberg, D. R., Hida, Y., Shimizu, A., Kaipainen, A., Kreuter, M., Kim, C. C., and Klagsbrun, M. (2004) Semaphorin 3F, a chemorepulsant for endothelial cells, induces a poorly vascularized, encapsulated, nonmetastatic tumor phenotype. *J. Clin. Invest. 114*, 1260−1271.

(12) Takahashi, T., and Strittmatter, S. M. (2001) Plexina1 autoinhibition by the plexin sema domain. *Neuron 29*, 429−439.

(13) Aci-Seche, S., Sawma, P., Hubert, P., Sturgis, J. N., Bagnard, D., Jacob, L., Genest, M., and Garnier, N. (2014) Transmembrane recognition of the semaphorin co-receptors neuropilin 1 and plexin A1: coarse-grained simulations. *PLoS One 9*, e97779.

(14) He, H., Yang, T., Terman, J. R., and Zhang, X. (2009) Crystal structure of the plexin A3 intracellular region reveals an autoinhibited conformation through active site sequestration. *Proc. Natl. Acad. Sci. U. S. A. 106*, 15610−15615.

(15) Bell, C. H., Aricescu, A. R., Jones, E. Y., and Siebold, C. (2011) A dual binding mode for RhoGTPases in plexin signalling. *PLoS Biol. 9*, e1001134.

(16) Wang, Y., He, H., Srivastava, N., Vikarunnessa, S., Chen, Y. B., Jiang, J., Cowan, C. W., and Zhang, X. (2012) Plexins are GTPase-activating proteins for Rap and are activated by induced dimerization. *Sci. Signaling 5*, ra6.

(17) Janssen, B. J., Robinson, R. A., Perez-Branguli, F., Bell, C. H., Mitchell, K. J., Siebold, C., and Jones, E. Y. (2010) Structural basis of semaphorin-plexin signalling. *Nature 467*, 1118−1122.

(18) Driessens, M. H., Hu, H., Nobes, C. D., Self, A., Jordens, I., Goodman, C. S., and Hall, A. (2001) Plexin-B semaphorin receptors

DOI: 10.1021/acs.biochem.6b00517
Biochemistry 2016, 55, 4928−4938

interact directly with active Rac and regulate the actin cytoskeleton by activating Rho. *Curr. Biol. 11*, 339−344.
(19) Zanata, S. M., Hovatta, I., Rohm, B., and Puschel, A. W. (2002) Antagonistic effects of Rnd1 and RhoD GTPases regulate receptor activity in Semaphorin 3A-induced cytoskeletal collapse. *J. Neurosci. 22*, 471−477.
(20) Barton, R., Palacio, D., Iovine, M. K., and Berger, B. W. (2015) A cytosolic juxtamembrane interface modulates plexin a3 oligomerization and signal transduction. *PLoS One 10*, e0116368.
(21) Sawma, P., Roth, L., Blanchard, C., Bagnard, D., Cremel, G., Bouveret, E., Duneau, J. P., Sturgis, J. N., and Hubert, P. (2014) Evidence for New Homotypic and Heterotypic Interactions between Transmembrane Helices of Proteins Involved in Receptor Tyrosine Kinase and Neuropilin Signaling. *J. Mol. Biol. 426*, 4099−4111.
(22) MacKenzie, K. R., Prestegard, J. H., and Engelman, D. M. (1997) A transmembrane helix dimer: structure and implications. *Science 276*, 131−133.
(23) Roth, L., Nasarre, C., Dirrig-Grosch, S., Aunis, D., Cremel, G., Hubert, P., and Bagnard, D. (2007) Transmembrane domain interactions control biological functions of neuropilin-1. *Mol. Biol. Cell 19*, 646−654.
(24) Palaisa, K. A., and Granato, M. (2007) Analysis of zebrafish sidetracked mutants reveals a novel role for Plexin A3 in intraspinal motor axon guidance. *Development 134*, 3251−3257.
(25) Birely, J., Schneider, V. A., Santana, E., Dosch, R., Wagner, D. S., Mullins, M. C., and Granato, M. (2005) Genetic screens for genes controlling motor nerve-muscle development and interactions. *Dev. Biol. 280*, 162−176.
(26) Schramm, C. A., Hannigan, B. T., Donald, J. E., Keasar, C., Saven, J. G., Degrado, W. F., and Samish, I. (2012) Knowledge-based potential for positioning membrane-associated structures and assessing residue-specific energetic contributions. *Structure 20*, 924−935.
(27) Su, P. C., and Berger, B. W. (2012) Identifying key juxtamembrane interactions in cell membranes using AraC-based transcriptional reporter assay (AraTM). *J. Biol. Chem. 287*, 31515−31526.
(28) Zhang, L., Polyansky, A., and Buck, M. (2015) Modeling transmembrane domain dimers/trimers of plexin receptors: implications for mechanisms of signal transmission across the membrane. *PLoS One 10*, e0121513.
(29) Jo, S., Kim, T., Iyer, V. G., and Im, W. (2008) Software news and updates - CHARNIM-GUI: A web-based grraphical user interface for CHARMM. *J. Comput. Chem. 29*, 1859−1865.
(30) Qi, Y. F., Ingolfsson, H. I., Cheng, X., Lee, J., Marrink, S. J., and Im, W. (2015) CHARMM-GUI Martini Maker for Coarse-Grained Simulations with the Martini Force Field. *J. Chem. Theory Comput. 11*, 4486−4494.
(31) Brooks, B. R., Brooks, C. L., III, Mackerell, A. D., Jr., Nilsson, L., Petrella, R. J., Roux, B., Won, Y., Archontis, G., Bartels, C., Boresch, S., Caflisch, A., Caves, L., Cui, Q., Dinner, A. R., Feig, M., Fischer, S., Gao, J., Hodoscek, M., Im, W., Kuczera, K., Lazaridis, T., Ma, J., Ovchinnikov, V., Paci, E., Pastor, R. W., Post, C. B., Pu, J. Z., Schaefer, M., Tidor, B., Venable, R. M., Woodcock, H. L., Wu, X., Yang, W., York, D. M., and Karplus, M. (2009) CHARMM: The Biomolecular Simulation Program. *J. Comput. Chem. 30*, 1545−1614.
(32) de Jong, D. H., Singh, G., Bennett, W. F. D., Arnarez, C., Wassenaar, T. A., Schafer, L. V., Periole, X., Tieleman, D. P., and Marrink, S. J. (2013) Improved Parameters for the Martini Coarse-Grained Protein Force Field. *J. Chem. Theory Comput. 9*, 687−697.
(33) Monticelli, L., Kandasamy, S. K., Periole, X., Larson, R. G., Tieleman, D. P., and Marrink, S. J. (2008) The MARTINI coarse-grained force field: Extension to proteins. *J. Chem. Theory Comput. 4*, 819−834.
(34) Vandrunen, R., Vanderspoel, D., and Berendsen, H. J. C. (1995) GROMACS: A software package and a parallel computer for molecular-dynamics. *Abstracts of Papers of the American Chemical Society*, Vol. *209*, No. 49-COMP, American Chemical Society, Washington, DC.
(35) Pronk, S., Pall, S., Schulz, R., Larsson, P., Bjelkmar, P., Apostolov, R., Shirts, M. R., Smith, J. C., Kasson, P. M., van der Spoel, D., Hess, B., and Lindahl, E. (2013) GROMACS 4.5: a high-throughput and highly parallel open source molecular simulation toolkit. *Bioinformatics 29*, 845−854.
(36) Berendsen, H. J. C., Postma, J. P. M., Vangunsteren, W. F., Dinola, A., and Haak, J. R. (1984) MOLECULAR-DYNAMICS WITH COUPLING TO AN EXTERNAL BATH. *J. Chem. Phys. 81*, 3684−3690.
(37) van der Spoel, D., and van Maaren, P. J. (2006) The origin of layer structure artifacts in simulations of liquid water. *J. Chem. Theory Comput. 2*, 1−11.
(38) Wassenaar, T. A., Pluhackova, K., Bockmann, R. A., Marrink, S. J., and Tieleman, D. P. (2014) Going Backward: A Flexible Geometric Approach to Reverse Transformation from Coarse Grained to Atomistic Models. *J. Chem. Theory Comput. 10*, 676−690.
(39) Jo, S., Kim, T., and Im, W. (2007) Automated builder and database of Protein/Membrane complexes for molecular dynamics simulations. *PLoS One 2*, e880.
(40) Jo, S., Kim, T., Iyer, V. G., and Im, W. (2008) CHARMM-GUI: A web-based graphical user interface for CHARMM. *J. Comput. Chem. 29*, 1859−1865.
(41) Jo, S., Lim, J. B., Klauda, J. B., and Im, W. (2009) CHARMM-GUI Membrane Builder for Mixed Bilayers and Its Application to Yeast Membranes. *Biophys. J. 97*, 50−58.
(42) Wu, E. L., Cheng, X., Jo, S., Rui, H., Song, K. C., Lee, J., Davila-Contreras, E. M., Qi, Y., Monje-Galvan, V., Venable, R. M., Klauda, J. B., and Im, W. (2014) CHARMM-GUI Membrane Builder Toward Realistic Biological Membrane Simulations. *J. Comput. Chem. 35*, 1997−2004.
(43) Phillips, J. C., Braun, R., Wang, W., Gumbart, J., Tajkhorshid, E., Villa, E., Chipot, C., Skeel, R. D., Kalé, L., and Schulten, K. (2005) Scalable molecular dynamics with NAMD. *J. Comput. Chem. 26*, 1781−1802.
(44) Steinbach, P. J., and Brooks, B. R. (1994) New spherical-cutoff methods for long-range forces in macromolecular simulation. *J. Comput. Chem. 15*, 667−683.
(45) Andersen, H. C. (1983) Rattle: A "velocity" version of the shake algorithm for molecular dynamics calculations. *J. Comput. Phys. 52*, 24−34.
(46) Feller, S. E., Zhang, Y., Pastor, R. W., and Brooks, B. R. (1995) Constant pressure molecular dynamics simulation: The Langevin piston method. *J. Chem. Phys. 103*, 4613−4621.
(47) Martyna, G. J., Tobias, D. J., and Klein, M. L. (1994) Constant pressure molecular dynamics algorithms. *J. Chem. Phys. 101*, 4177−4189.
(48) Klauda, J. B., Venable, R. M., Freites, J. A., O'Connor, J. W., Tobias, D. J., Mondragon-Ramirez, C., Vorobyov, I., MacKerell, A. D., and Pastor, R. W. (2010) Update of the CHARMM all-atom additive force field for lipids: Validation on six lipid types. *J. Phys. Chem. B 114*, 7830−7843.
(49) Huang, J., and MacKerell, A. D. (2013) CHARMM36 all-atom additive protein force field: Validation based on comparison to NMR data. *J. Comput. Chem. 34*, 2135−2145.
(50) Durell, S. R., Brooks, B. R., and Bennaim, A. (1994) Solvent-Induced Forces between Two Hydrophilic Groups. *J. Phys. Chem. 98*, 2198−2202.
(51) Jorgensen, W. L., Chandrasekhar, J., Madura, J. D., Impey, R. W., and Klein, M. L. (1983) Comparison of Simple Potential Functions for Simulating Liquid Water. *J. Chem. Phys. 79*, 926−935.
(52) Brooks, B. R., Bruccoleri, R. E., Olafson, B. D., States, D. J., Swaminathan, S., and Karplus, M. (1983) CHARMM - a Program for Macromolecular Energy, Minimization, and Dynamics Calculations. *J. Comput. Chem. 4*, 187−217.
(53) Humphrey, W., Dalke, A., and Schulten, K. (1996) VMD: Visual molecular dynamics. *J. Mol. Graphics 14*, 33−38.
(54) Zhang, L., Sodt, A. J., Venable, R. M., Pastor, R. W., and Buck, M. (2013) Prediction, refinement, and persistency of transmembrane helix dimers in lipid bilayers using implicit and explicit solvent/lipid

DOI: 10.1021/acs.biochem.6b00517
Biochemistry 2016, 55, 4928−4938

representations: Microsecond molecular dynamics simulations of ErbB1/B2 and EphA1. *Proteins: Struct., Funct., Genet. 81*, 365−376.
(55) Zhang, J., and Lazaridis, T. (2009) Transmembrane Helix Association Affinity Can Be Modulated by Flanking and Noninterfacial Residues. *Biophys. J. 96*, 4418−4427.
(56) Feldner, J., Reimer, M. M., Schweitzer, J., Wendik, B., Meyer, D., Becker, T., and Becker, C. G. (2007) PlexinA3 restricts spinal exit points and branching of trunk motor nerves in embryonic zebrafish. *J. Neurosci. 27*, 4978−4983.
(57) Smith, A. W., Marita, M., Shi, X. J., and Comar, W. D. (2015) Decoding the Role of Receptor Dimerization in Plexin-Semaphorin Signaling. *Biophys. J. 108*, 257a−257a.
(58) Lemmon, M. A., Flanagan, J. M., Treutlein, H. R., Zhang, J., and Engelman, D. M. (1992) Sequence specificity in the dimerization of transmembrane alpha-helices. *Biochemistry 31*, 12719−12725.
(59) Russ, W. P., and Engelman, D. M. (2000) The GxxxG motif: a framework for transmembrane helix-helix association. *J. Mol. Biol. 296*, 911−919.
(60) Senes, A., Gerstein, M., and Engelman, D. M. (2000) Statistical analysis of amino acid patterns in transmembrane helices: the GxxxG motif occurs frequently and in association with beta-branched residues at neighboring positions. *J. Mol. Biol. 296*, 921−936.
(61) Mueller, B. K., Subramaniam, S., and Senes, A. (2014) A frequent, GxxxG-mediated, transmembrane association motif is optimized for the formation of interhelical Calpha-H hydrogen bonds. *Proc. Natl. Acad. Sci. U. S. A. 111*, E888−895.
(62) Burke, C. L., Lemmon, M. A., Coren, B. A., Engelman, D. M., and Stern, D. F. (1997) Dimerization of the p185neu transmembrane domain is necessary but not sufficient for transformation. *Oncogene 14*, 687−696.
(63) Berger, B. W., Kulp, D. W., Span, L. M., DeGrado, J. L., Billings, P. C., Senes, A., Bennett, J. S., and DeGrado, W. F. (2010) Consensus motif for integrin transmembrane helix association. *Proc. Natl. Acad. Sci. U. S. A. 107*, 703−708.
(64) Kong, Y., Janssen, B. J. C., Malinauskas, T., Vangoor, V. R., Coles, C. H., Kaufmann, R., Ni, T., Gilbert, R. J. C., Padilla-Parra, S., Pasterkamp, R. J., and Jones, E. Y. (2016) Structural Basis for Plexin Activation and Regulation. *Neuron 91*, 548−560.
(65) Deng, W., Cho, S., Su, P. C., Berger, B. W., and Li, R. (2014) Membrane-enabled dimerization of the intrinsically disordered cytoplasmic domain of ADAM10. *Proc. Natl. Acad. Sci. U. S. A. 111*, 15987−15992.
(66) Oates, J., King, G., and Dixon, A. M. (2010) Strong oligomerization behavior of PDGFbeta receptor transmembrane domain and its regulation by the juxtamembrane regions. *Biochim. Biophys. Acta, Biomembr. 1798*, 605−615.
(67) Matsushita, C., Tamagaki, H., Miyazawa, Y., Aimoto, S., Smith, S. O., and Sato, T. (2013) Transmembrane helix orientation influences membrane binding of the intracellular juxtamembrane domain in Neu receptor peptides. *Proc. Natl. Acad. Sci. U. S. A. 110*, 1646−1651.
(68) Su, P. C., and Berger, B. W. (2013) A novel assay for assessing juxtamembrane and transmembrane domain interactions important for receptor heterodimerization. *J. Mol. Biol. 425*, 4652−4658.

DOI: 10.1021/acs.biochem.6b00517
Biochemistry 2016, 55, 4928−4938